PHYSICAL REVIEW B VOLUME 51, NUMBER 19 15 MAY 1995-I

Mesoscopic mechanisms of the photovoltaic effect and microwave absorption in granular metals

B. Spivak and F. Zhou
Physics Department, University of Washington, Seattle, Washington 98195

M. T. Beal Monod
Physique des Solides, Universite de Paris–Sud, 91405, Orsay Cedex, France

(Received 21 September 1994; revised manuscript received 24 January 1995)

A theory for the photovoltaic current and microwave absorption in mesoscopic samples is developed. The photovoltaic current is determined by the displacement of the center of mass of the electronic wave function produced by inelastic electron transitions. At low frequencies the main contribution to the microwave conductivity of isolated mesoscopic samples is shown to be due to a relaxation mechanism which resembles the Mandelstam-Leontovich sound-absorption mechanism in gases and the Pollak-Geballe conductivity mechanism in doped semiconductors. A giant positive magnetoresistance in granular metals is predicted.

I. INTRODUCTION

The irradiation of a sample without an inversion center by electromagnetic waves can cause a direct current flow. This is known as the photovoltaic effect. Random distribution of impurities in mesoscopic samples leads to symmetry breaking[1,2] and to the existence of a photovoltaic current. For the case of microwave irradiation, a theory of this effect was given in Ref. 3, where the contribution from direct photon absorption was taken into account. The amplitude of the photovoltaic current I_{PV} found in Ref. 3 was inversely proportional to the irradiation frequency ω and negligibly small at high ω. This is due to the fact that the contribution to I_{PV} from transitions between electron states with different energies cancel each other, and the effectiveness of the cancellation increases with ω. Another reason for the decreasing of I_{PV} with ω is that at large ω transitions take place between electron states with large inelastic broadening.

In this paper we consider a new mechanism which at high ω leads to a frequency-independent photovoltaic current and makes a larger contribution compared with Ref. 3 to the current at high ω, for example in the case of laser irradiation. At low ω this mechanism can also dominate the photovoltaic current in the case of isolated mesoscopic samples. Finally we will show that the same mechanism can dominate the microwave absorption and lead to a gigantic positive magnetoresistance in granular metals.

II. PHOTOVOLTAIC CURRENT AT HIGH FREQUENCY OF IRRADIATION

Let us consider the situation when a nonequilibrium distribution of electrons is created in metal due to light illumination. In the absence of a magnetic field, the electron wave function can be chosen as real and representing zero current. In a disordered system of finite size, the wave functions which correspond to different energies have centers of mass located at random positions. The relaxation of the nonequilibrium electron distribution created by the light leads to inelastic transitions between states with different energies, and to shifts of the electronic centers of mass in random directions. This leads to a photovoltaic current I_{PV}, which flows in a random, sample-specific direction. In other words, a nonzero value of I_{PV} arises only when nondiagonal elements of the density matrix representing the transitions between different energies are taken into account. This effect is beyond the Boltzmann equation approximation. In crystals with no inversion symmetry this effect was considered in Ref. 4.

To calculate the current we use the Keldysh diagram technique, with matrix-type Green's functions

$$G_\epsilon(\mathbf{r},\mathbf{r}')=\begin{bmatrix} G_\epsilon^R(\mathbf{r},\mathbf{r}') & G_\epsilon^K(\mathbf{r},\mathbf{r}') \\ 0 & G_\epsilon^A(\mathbf{r},\mathbf{r}') \end{bmatrix} . \tag{1}$$

Here $G_\epsilon^{A(R,K)}(\mathbf{r},\mathbf{r}')$ represent the advanced, retarded, and Keldysh Green's functions, respectively.

The equation for the current density has the form

$$J(\mathbf{r})=\frac{eh}{2m}\mathrm{Im}\int d\epsilon(\partial_{\mathbf{r}}-\partial_{\mathbf{r}'})G_\epsilon^K(\mathbf{r},\mathbf{r}')_{\mathbf{r}-\mathbf{r}'} . \tag{2}$$

We consider the sample geometries shown in Fig. 1 with width L_y, thickness L_z, and length L_x, and assume that $L_x,L_y,L_z \gg l$, where l is elastic electron mean free path.

Using the second-order correction of the perturbation theory for $G_\epsilon^K(\mathbf{r},\mathbf{r}')$ due to electron-phonon interaction, which is given by the diagram shown in Fig. 2, we obtain the expression for the photovoltaic current in the x direction:

$$I_{\mathrm{PV}}=\frac{e(V\nu)^2}{L_x}\int d\epsilon\, d\epsilon' W_{\epsilon,\epsilon'}[X_\epsilon - X_{\epsilon'}] , \tag{3}$$

where

$$X_\epsilon=\frac{\int d\mathbf{r}\, \nu_\epsilon(\mathbf{r})x}{V\nu} \tag{4}$$

0163-1829/95/51(19)/13226(5)/$06.00

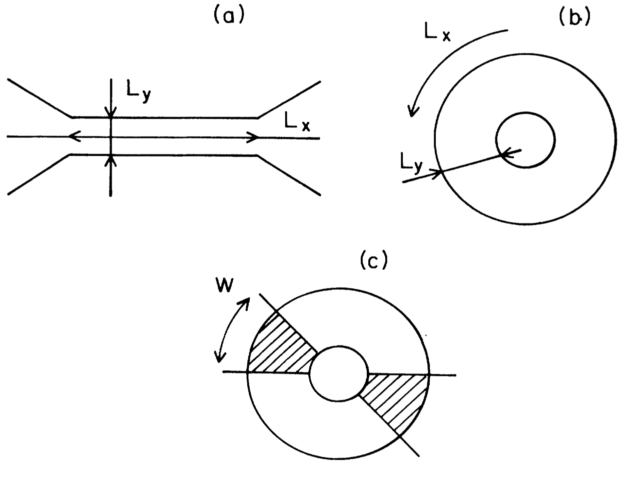

FIG. 1. Sample geometries.

is the x coordinate of the center of mass of the electron wave function at energy ϵ, V is the sample volume, $\nu_\epsilon(\mathbf{r})=\mathrm{Im}G^R_\epsilon(\mathbf{r},\mathbf{r}')$ is the local density of states at the point $\mathbf{r}$, $\nu_\epsilon=[\int \nu_\epsilon(\mathbf{r})dr/V]$, and $\nu=\langle\nu_\epsilon\rangle$. Here the brackets $\langle\ \rangle$ represent the averaging over random potential realizations, and $W_{\epsilon,\epsilon'}$ is the rate of inelastic electron transitions between states with energies ϵ and ϵ'. Both electron-electron and electron-phonon scatterings contribute to $W_{\epsilon,\epsilon'}$. We neglect the mesoscopic fluctuations of $W_{\epsilon,\epsilon'}$.

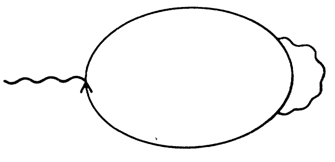

FIG. 2. The diagram describing G_K. Solid and wavy lines correspond to electron and phonon Green functions.

As we have mentioned, $\langle I_{\mathrm{PV}}\rangle=0$. To estimate the typical value of the current we calculate the variance of the photovoltaic current,

$$\langle I^2_{\mathrm{PV}}\rangle=\frac{e^2(V\nu)^4}{L_x^2}\int d\epsilon\, d\epsilon' d\epsilon_1 d\epsilon_1' W_{\epsilon,\epsilon'}W_{\epsilon_1,\epsilon_1'} \times\langle \delta X_{\epsilon,\epsilon'}\delta X_{\epsilon_1,\epsilon_1'}\rangle\ . \tag{5}$$

Here $\delta X_{\epsilon,\epsilon'}=X_\epsilon-X_{\epsilon'}$.

In the weak-scattering limit $p_F l\gg 1$ (p_F is the Fermi momentum), the correlation function of $\langle X_\epsilon,X_{\epsilon'}\rangle$ can be calculated with the help of the diagrams in Fig. 3 which have been used to calculate the fluctuations of the density of states in mesoscopic metals in Ref. 5:

$$\langle X_\epsilon X_{\epsilon'}\rangle=(V\nu)^{-2}\int\int d\mathbf{r}\, d\mathbf{r}' xx'\mathrm{Re}\{P^C_{\epsilon-\epsilon'}(\mathbf{r},\mathbf{r}')^2 +P^D_{\epsilon-\epsilon'}(\mathbf{r},\mathbf{r}')^2\} \tag{6}$$

Cooperons and diffusions $P^{C,D}_{\epsilon-\epsilon'}(\mathbf{r},\mathbf{r}')$ are described by equations[1,2]

$$\left\{i\omega+ie[U'(\mathbf{r})-U(\mathbf{r}')]+D\left[i\hbar\partial_{\mathbf{r}}-\frac{\mathbf{e}}{c}[A(\mathbf{r})\pm\mathbf{A}'(\mathbf{r}')]\right]^2+1/\tau_\epsilon\right\}P^{C,D}_\omega(\mathbf{r},\mathbf{r}')=\delta(\mathbf{r}-\mathbf{r}')\ . \tag{7}$$

Here $U(\mathbf{r})$ and $\mathbf{A}(\mathbf{r})$ are scalar and vector potentials, respectively.

As a result, in the absence of a magnetic field we have

$$\langle X_\epsilon X_{\epsilon'}\rangle=\sum_{n_x=1}^{\infty}\sum_{m_x,m_y,m_z=0}^{\infty}\frac{1}{n_x^2}\mathrm{Re}\left\{\frac{L_x^2\Delta^2}{(n_x-m_x)^2E_{cx}+m_y^2E_{cy}+m_z^2E_{cz}+i(\epsilon-\epsilon')+\dfrac{1}{\tau_\epsilon}} \times\frac{1}{m_x^2E_{cx}+m_y^2E_{cy}+m_z^2E_{cz}+i(\epsilon-\epsilon')+\dfrac{1}{\tau_\epsilon}}\right\}\ . \tag{8}$$

Here we introduce $E_{ci}=D/L_i^2$, where L_i is the size of the sample along the i direction with $i=x$, y, and z, D is the diffusion coefficient, $\Delta=1/\nu V$ is the level spacing, and τ_ϵ is the electron energy relaxation time. It follows from Eq. (8) that the typical $\delta X_{\epsilon,\epsilon'}$ vanishes when $|\epsilon-\epsilon'|\ll 1/\tau_\epsilon$, and saturates when $\epsilon-\epsilon'\gg 1/\tau_\epsilon$ at the value

$$\delta X_{\epsilon,\epsilon'}\sim\frac{L_x}{\sqrt{G_{0x}}}\sqrt{\Delta\tau_\epsilon}\ . \tag{9}$$

Here $G_{0i}=G_i h/e^2\sim E_{ci}/\Delta$, and G_i is the conductance of the sample when an external voltage is applied along the i direction. In the dielectric regime, where $G_{0i}\ll 1$ and the electron wave functions are localized, the typical distance in the x direction between the centers of mass of two arbitrary eigenstates is of the order of L_x. This is in agreement with Eq. (9), which also gives $|X_\epsilon-X_{\epsilon'}|\sim L_x$ at $G_{0x}\sim 1$.

In this paper we consider the simplest case, in which the laser illumination of the sample leads to overheating of the electron subsystem with respect to the phonon. This happens when $\tau_e\ll\tau_{\mathrm{ph}}$, where τ_e, τ_{ph} are the electron-electron and electron-phonon relaxation times

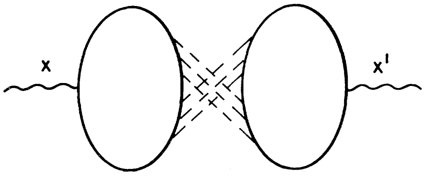

FIG. 3. The diagram describing $\langle \delta X_\epsilon \delta X_{\epsilon'} \rangle$. Solid lines correspond to the electron Green function, and dashed lines correspond to impurity scatterings.

$[1/\tau_\epsilon = (1/\tau_e) + (1/\tau_{\text{ph}})]$. In this case, nonequilibrium electrons are created with large energies and then, due to a cascade of electron-electron scatterings, they are transferred into the region of energy of order T^* and finally emit phonons. We assume that the phonon mean free path is larger than the sample thickness, and that the phonon subsystem has an equilibrium distribution function N_ϵ with the same temperature as the temperature of the bath T_0. In this case the electron subsystem can be characterized by an effective temperature T^* which does not depend on ω and is governed by the energy conservation equation $[T^*(T^* - T_0)V]/\tau_{\text{ph}} = Q$, where Q is the energy dissipation rate of the sample. Typically at helium temperatures the overheating $(T^* - T_0)$ is of the order of 1° per 1 W/sm^2.

Due to detailed balance, the electron-electron scattering does not contribute to $W_{\epsilon,\epsilon'}$ in this case, and we have the standard expression for the electron-phonon-scattering integral

$$W_{\epsilon,\epsilon'} = \frac{1}{\tau_{\epsilon,\epsilon'}} \{ n_\epsilon (1 - n_\epsilon) N_{\epsilon - \epsilon'} - n_{\epsilon'} (1 - n_\epsilon) [1 + N_{\epsilon - \epsilon'}] \} , \quad (10)$$

where $\tau_{\epsilon,\epsilon'}$ is the mean electron transition time from ϵ to ϵ' due to electron-phonon interaction. As a result, we can estimate the variance of the photovoltaic current, for example, for the ring geometry shown in Fig. 1(b),

$$\sqrt{\langle \overline{I_{\text{PV}}^2} \rangle} = \gamma e \Delta \frac{(T^* - T_0)}{T^*} \left[\frac{1}{E_{cx} \tau_\epsilon (T^*)} \right]^{1/2} . \quad (11)$$

Here $\overline{I_{\text{PV}}}$ means averaging over the oscillation period of the external field, γ is the constant of order of unity, and $\tau_\epsilon(T^*)$ is the relaxation time at the temperature T^*. Equation (11) holds, provided $L_\epsilon = \sqrt{D\tau_\epsilon} \gg L_x, L_y, L_z$.

In typical situations the photovoltaic current [Eq. (11)] turns out to be smaller than measured in[6,7] equilibrium persistent current. We think, however, that it can be observed experimentally.

In a bulk isolated mesoscopic sample the total current through the sample is zero, but the magnetic moment generated by the local photovoltaic current densities should be of the same order $M \sim L_x L_y \sqrt{\langle \overline{I_{\text{PV}}^2} \rangle}$ as of the ring geometry case Fig. 1(b). Equation (11) does not depend on ω (while resonant photon absorption[3] makes a decreasing contribution to I_{PV} with increasing ω), and makes the main contribution to I_{PV} at high frequencies $\omega \gg T^*$. The physical reason for the ω independence of Eq. (11) is that it is determined by electron-phonon relaxation processes with a typical energy transfer of the order of T^*.

The magnetic-field dependence of the photovoltaic current exhibits the usual random oscillations for mesoscopic samples,[1,2] which can be calculated using Eq. (7). The characteristic period of these oscillations, for example, in the case of the ring geometry Fig. 1(b) is $H_c \sim \Phi_0 / L_\epsilon^2$ (Φ_0 is the flux quantum). We assume that the magnetic field is applied in the z direction.

At low frequencies we can distinguish two cases. (a) The mesoscopic part of a sample is connected to the bulk by leads which are used to measure the photovoltaic current. The oscillating electric field is applied between the leads as in Fig. 1(a). In this case, the theory developed in Ref. 3 accounts for the dominant contribution to the photovoltaic current. (b) The sample is electrically isolated [Fig. 1(b)], and the photovoltaic current is measured by measuring the magnetic moment associated with the photovoltaic current, similar to Refs. 6 and 7. In this case, the mechanism presented above will dominate the current even at low frequencies. The same situation will also arise in case (a), when the oscillating electric field is applied perpendicular to the direction between the leads to the direction of the photovoltaic current. In Sec. III we consider this situation in more detail.

III. THE MICROWAVE ABSORPTION AND PHOTOVOLTAIC CURRENT AT LOW FREQUENCY

We start with a discussion of microwave absorption in a system of isolated disordered metallic grains at low temperature. (We will assume, however, that $\Delta \ll 1/\tau_\epsilon$). This situation has been considered in many papers (see, for example, Refs. 8 and 9), which concluded that the dominant mechanism for microwave absorption involves resonant transitions between electron levels. In the limit $\Delta \gg 1/\tau_\epsilon$, this leads to the classical expression for the conductivity $\sigma_{\text{cl}} = \omega^2 / \sigma_D$ where $\sigma_D = e^2 \nu D$ is the Drude conductivity. The contribution from this mechanism was calculated with the help of the Kubo formula, which corresponds to resonance transitions between one-particle electron states in an oscillating electric field.

We show below, however, that the relaxation mechanism can dominate the microwave absorption in mesoscopic samples. This mechanism resembles the Mandelstam-Leontovich sound-absorption mechanism and second viscosity in gases,[10] and the Pollak-Geballe microwave absorption mechanism in doped semiconductors.[11]

A qualitative picture of the mechanism is as follows. The density of states $\nu(\epsilon)$ of an isolated disordered metallic sample exhibits sample-specific fluctuations as a function of energy. These fluctuations are sensitive to the external electric field. This is because different electron energy levels are moved by external field in random directions. As a result, at low ω the density of states oscillates in time with the same frequency as the external electric field. The population of the energy levels in this case adiabatically follows their motion. As a result, a nonequilibrium distribution of electrons is created. Relaxation of the nonequilibrium distribution due to inelastic processes leads to entropy production and to the absorption of the energy from the external field.

In this case the equation for the distribution function of electrons is

$$\partial_t \delta f(\epsilon,t) = -\delta f(\epsilon,t)/\tau_\epsilon + \partial_\epsilon n(\epsilon,t) \int_{-\infty}^{\epsilon} d\epsilon' \partial_t \nu_{\epsilon'}(U(t)) \ . \tag{12}$$

Here $\nu_\epsilon(U(t))$ is the density of states at time t, and $U(t)$ is the voltage applied in the z direction: $\delta f(\epsilon,t) = f(\epsilon,t) - f_{\text{eq}}(\epsilon,t)$, $f(\epsilon,t) = \nu_\epsilon(U(t)) n(\epsilon,t)$, and $f(\epsilon,t)_{\text{eq}} = \nu_\epsilon(U(t)) n_F(\epsilon)$, where $n_F(\epsilon)$ is the equilibrium Fermi distribution function. The second term in Eq. (12) describes the creation of a nonequilibrium distribution of electrons due to the motion of the energy levels in the external electric field. This equation neglects the possible nonuniformity of f as a function of $\mathbf{r}$, and holds if $E_c \gg (1/\tau_\epsilon), \omega$. It can be derived by using Keldysh diagram technique and calculating the diagram in Fig. 2. We assume that the electric field is parallel to the z direction.

It is important to note that the inelastic transitions that relax the nonequilibrium distribution function correspond to the energy transfer of the order of ϵ itself, in spite of the fact that the electron energy levels are shifted by the external electric field only by small amounts. This is because $(\tau_{\epsilon-\epsilon'})^{-1} \sim (\epsilon-\epsilon')^2$, and transitions with small $|\epsilon-\epsilon'|$ have small probabilities. That is why we can use the relaxation-time approximation in Eq. (12).

As a result, the conductance of the sample averaged over random potential configurations has the form

$$G_\omega = \frac{\omega^2 \tau_\epsilon}{1+(\omega\tau_\epsilon)^2} T_0 V \nu^{-1} \int d\epsilon (\partial_\epsilon n_F(\epsilon))^2 \int_{-\infty}^{\epsilon} \int_{-\infty}^{\epsilon} d\epsilon_1 d\epsilon_2 \partial_U \partial_{U'} \langle \nu_{\epsilon_1}(U) \nu_{\epsilon_2}(U') \rangle_{U' \to U} \ . \tag{13}$$

Taking into account the penetration of the electric field into the sample only up to the screening length r_0, and calculating the correlation function $\langle \partial_U \nu_{\epsilon_1}(U) \partial_U \nu_{\epsilon_2}(U) \rangle$ with the help of the diagrams in Fig. 3, we obtain

$$G_\omega = \frac{(\omega\tau_\epsilon)^2}{1+(\omega\tau_\epsilon)^2} \frac{e^2}{\hbar G_{0z}} \frac{r_0^2}{L_z^2} \ . \tag{14}$$

It is important to note that at low ω the mechanism considered above makes a larger contribution to G_ω than the classical one $\sigma_{\text{cl}}(L_x L_y / L_z)$, provided

$$(E_F \tau_\epsilon)^2 \left[\frac{r_0 h}{p_F L_y L_z} \right]^2 \gg 1 \ . \tag{15}$$

As we have mentioned, Eqs. (14) and (15) hold when $1/\tau_\epsilon \gg \Delta$. In the opposite limit the calculation of G_ω must be based on the Wigner-Dyson ensemble theory for the electron-energy-level distribution.[13] In this case, the mechanism considered above also dominates the microwave absorption at low ω. However, the quantitative calculation of G_ω in this case requires knowledge of $X_\epsilon - X_{\epsilon'}$ and the picture of the electric field screening in the situation when $1/\tau_\epsilon \ll |\epsilon-\epsilon'| \ll \Delta$. In this region the diagrammatic technique employed above does not work.

It follows from Eqs. (13) and (7) that G_ω exhibits a gigantic positive magnetoresistance which is due to magnetic-field suppression of the mesoscopic fluctuations density of states (see Refs. 5 and 12). For $\Phi \ll \Phi_0$ we obtain

$$G_\omega(H) = \frac{G_\omega(0)}{2} \left[1 + \frac{1}{1+\tau_\epsilon \sqrt{E_{cx} E_{cy}} \left[\frac{\Phi}{\Phi_0} \right]^2} \right] \ . \tag{16}$$

Here Φ is the magnetic flux through the sample in the z direction. Equation (16) predicts that the characteristic magnetic field required to reduce G_ω by a factor 2 is of the order of H_c. Note that this corresponds to the situation where the flux through the sample is much less than 1. Furthermore for the mesoscopic ring case the conductance is a periodic function of a half-flux quantum, with the relative amplitude of the order of 1. Even if $(E_F \tau_\epsilon)^2 (r_0 h / p_F L_x L_y)^2 \ll 1$ and the classical contribution dominates the value of G_ω, the magnetoresistance can still be determined by the effect considered above, provided $(E_F \tau_\epsilon)^2 (h r_0 / p_F L_x L_y)^2 G_{0z} \gg 1$. We get this estimate by comparing Eq. (16) with the weak-localization corrections to σ_D obtained in Ref. 12.

The sign of the magnetoresistance $G_\omega(H)$ considered above is the same as the sign of the weak-localization corrections to σ_D corresponding to the negative magnetoresistance.[12] We would like to mention, however, that the nature of the giant magnetoresistance considered above is different from the weak-localization corrections, which are small at $p_F l \ll 1$. The other difference is that the sign of the magnetoresistance considered above does not depend on the presence of spin-orbit scattering.

Let us now turn to the case of the photovoltaic current. As we have discussed above, the inelastic electron transitions correspond to displacements of the center of mass of electron wave functions. As a result, we have

$$\sqrt{\langle \overline{I_{\text{PV}}^2} \rangle} = \frac{e}{\hbar} Q_x(\omega) \tau_\epsilon \frac{\Delta}{T_0} \frac{1}{\sqrt{G_{0x} \tau_\epsilon \Delta}} \ , \tag{17}$$

which is larger than the corresponding expression for resonance absorption.[3] Here $Q_x(\omega) = G_\omega \overline{U^2(t)}$, and we assume that the external ac field is applied along the z direction. Equation (17) gives $\sqrt{\langle \overline{I_{\text{Pv}}^2} \rangle} \sim \omega^2$, which is valid at arbitrary small ω.

There are, however, cases when at asymptotically low frequencies $\sqrt{\langle \overline{I_{\text{PV}}^2} \rangle} \sim |\omega|$. This occurs when the external electric potential cannot be represented in the form $U(\mathbf{r},t) = F(\mathbf{r}) G(t)$, where F and G are arbitrary functions. The experimental realization of this situation can be achieved, for example, by a disordered metallic ring

[Fig. 1(c)] which is separated from the gates by a dielectric, when voltages on the gates $U_1(t)$, and $U_2(t)$ are arbitrary periodical functions with the same period and different initial phases. The requirement for the dc photovoltaic current not to be zero in this case is that the area A_{U_1,U_2} which is enclosed by the path in configuration space $\{U_1(t), U_2(t)\}$ is not zero. Solving Eq. (12), we get

$$\sqrt{\langle \overline{I_{\mathrm{PV}}}^2 \rangle} \sim e|\omega| N \ . \tag{18}$$

Here $\overline{I_{\mathrm{PV}}}$ is the current along the ring averaged over a period

$$N = \frac{\Delta \tau_\epsilon}{T G_{0x}} \sqrt{A_{U_1,U_2}} \ . \tag{19}$$

Here we assume that the width of the gates in the Fig. 1(c) is of the order of L_x, $L_i \ll L_T$. In the case when the differences between the initial phases of U_1 and U_2 is of the order of π and $U_1 \sim U_2 \sim U_0$ we estimate $A_{U_1,U_0} \sim \overline{(U_0(t))^2}$. In the case of disordered metallic samples from Eq. (19) we have $N \ll 1$. However, we think that in the case of semiconductor ballistic quantum dots it is possible to have $N \sim 1$.

The origin of the current calculated above [Eq. (18)] is similar to that in experiments on the electron pumping in granular metals.[14]

The sensitivity of this effect to the magnetic field is the same as stated above [Eq. (16)].

ACKNOWLEDGMENTS

We have greatly benefited from the discussion with B. Altshuler, H. Bouchiat, Y. Gefen, B. Shklovski, and D. Thouless. This work was partially supported by the Division of Material Sciences, National Science Foundation, under Contract No. DMR-9205144. One of us (B.S.) gratefully acknowledges the hospitality and support of the Université de Paris–Sud at Orsay.

---

[1] P. Lee and A. D. Stone, Phys. Rev. Lett. **55**, 1622 (1985).

[2] B. Altshuler and D. Khmelnitskii, Pisma. Zh. Eksp. Teor. Fiz. **42**, 291 (1985) [JETP Lett. **42**, (1985)].

[3] V. I. Fal'ko and Khmel'nitskii, Zh. Eksp. Teor. Fiz. **95**, 328 (1989) [Sov. Phys. JETP **68**, 186 (1989)].

[4] V. I. Belinicher, E. L. Ivchenko, and B. I. Sturman, Zh. Eksp. Teor. Fiz. **83**, 649 (1982) [Sov. Phys. JETP **56**, 359 (1982)].

[5] B. Altshuler and B. Shklovskii, Zh. Eksp. Teor. Fiz. **91**, 220 (1986) [Sov. Phys. JETP **64**, 127 (1986)].

[6] L. Levy, G. Dolan, J. Dunsmuir, and H. Bouchiat, Phys. Rev. Lett. **64**, 2074, 1990; L. Levy, Physica B **169**, 245 (1991).

[7] V. Chandrasekhar, R. Webb, M. Brady, M. Ketchen, W. Gallagher, and A. Kleinsasser, Phys. Rev. Lett. **67**, 3578 (1991).

[8] J. Perenboom, P. Wyder, and F. Meier, Phys. Rep. **78**, 173 (1981); G. Carr, S. Percowitz, and X. Tanner, in *Far Infrared Properties of Inhomogeneous Materials,* edited by K. Button (Academic, Orlando, FL, 1984), Vol. 15.

[9] B. I. Shklovskii, Pisma Zh. Eksp. Teor. Fiz. **36**, 287 (1982) [Sov. Phys. JETP **36**, 352 (1982)]; L. P. Gorkov and G. M. Eliashberg, *ibid.* **48**, 1407 (1965) [*ibid.* **21**, 940 (1965)]; D. Mast and R. Serota, Phys. Rev. B **41**, 7850 (1990).

[10] L. D. Landau and E. M. Lifshitz, *Fluid Mechanics* (Pergamon, Oxford, 1977).

[11] M. Pollak and T. H. Geballe, Phys. Rev. **122**, 1742 (1961).

[12] B. I. Altshuler and P. A. Lee, Phys. Rev. B **19**, 1548 (1979).

[13] K. B. Efetov, Adv. Phys. **32**, 2 (1983).

[14] H. Pothierf, P. Lafarge, C. Urbina, D. Esteve, and M. Devoret, Europhys. Lett. **17**, 249 (1992).